ACADEMIA ROMÂNĂ
Revue Roumaine de Chimie
http://web.icf.ro/rrch/

Rev. Roum. Chim.,
2018, *63*(11), 1043-1051

PALLADIUM(II) COMPLEXES BASED ON SCHIFF BASE LIGANDS: SYNTHESIS, CHARACTERIZATION, DNA BINDING, ANTI-BACTERIAL AND ANTI α-GLUCOSIDASE ACTIVITY

Uzma ALI, Syed Ahmed TIRMIZI,* Muhammad Babar TAJ* and Ahmad RAHEEL

Department of Chemistry, Quaid-e-Azam University Islamabad, 44000, Pakistan

Received December 11, 2017

This article describes the synthesis of three Pd(II) complexes regarding bidentate Schiff base ligands, namely $[Pd(L_1)_2]$ (1), $[Pd(L_2)_2]$ (2), $[Pd(L_3)_2]$ (3) [**HL_1** = 2-(((2-mercaptophenyl)imino)methyl)naphthalen-1-ol, **HL_2** = (E)-2-((4-chlorobenzylidene)amino)naphthalen-1-ol, **HL_3** = 3-((4-chlorobenzylidene)amino)-4-hydroxy-5-nitrobenzenesulfonic acid]. All the compounds were characterized by elemental analysis, FT-IR, multi nuclear NMR (^{1}H and ^{13}C) and UV-vis absorption spectra. Palladium complexes and Schiff bases were investigated as DNA binding, antibacterial and anti α-glucosidase agents against four human pathogenic bacteria.

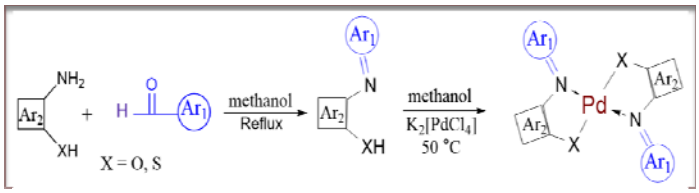

INTRODUCTION

Schiff base is a very famous moiety in chemistry specially which contain aryl substituents are more stable and more easily synthesized. Schiff base ligands that are able to form transition metal coordination compounds are intermediate between structural and magnetic exchange interactions[1] and different enzymes and proteins.[2] The complexes thus exhibit the important role in coordination chemistry linked to magnetism, catalysis and bioinorganic modeling studies.[3] In this respect, there is much passion in designing bi-nucleating ligands and their transition metal coordination compounds. Metal ions play an essential part in living system, both in development and in metabolism. The active sites of a large number of the biomolecules[4] are coordination complexes including one or more metal ions. The potential relation with those of synthetic coordination complexes has contributed importantly to the development of the interdisciplinary field of bioinorganic chemistry.[5] The bioinorganic chemistry forms the molecular foundation of all possible interactions between the biological molecules and metal ions which is in turn enforced in the study of medicine, environmental sciences, biology, technology and catalysis. Cooperation of several metal ions with antibiotics may increase or decrease their antimicrobial activity but mostly in many cases the pharmacological action of antibiotics after complexation with metals is increased as compared to free ligands.[6] Broadly speaking it has been noted that transition metal complexes have less toxicity and greater activity as compared to ligand alone. Palladium metal is very attractive for metallodrugs because it exhibits structural houses much like those of platinum and also parade auspicious *in vitro* cytotoxicity.[7-9] Palladium metal is very attractive for metallodrugs because it exhibits structural houses much like those of platinum and also parade auspicious *in vitro* cytotoxicity. The antiviral and antibacterial behavior of different palladium (II) complexes

* Corresponding authors drbabartaj@gmail.com , mbtaj@chem.qau.edu.pk , satirmizi_qau@yahoo.com

with various kinds of ligands at the growth and metabolism of numerous colonies of microorganisms has been considered and described.[10] All the study justifies that the synthesis and characterization of new metal complexes as a DNA binding, anti-bacterial and anti α-glucosidase agent are of extreme value to consider the drug-metal ion coupling and to study their impressive applications in pharmacological field.

EXPERIMENTAL

Materials and Chemicals

All the chemicals used for synthesis were pure. Solvents were of AR grade and were purified and dried by standard procedures. Metal salts were purchased from Merck. 2-aminothiophenol, 2-hydroxynaphthaldehyde, 4-chloro-benzaldehyde were obtained from Aldrich. Ethanol, Methanol, DMSO were used as solvents purchased from Sigma Aldrich. Melting points were determined on Gallon Kamp melting point apparatus using open capillaries and were uncorrected. The solution conductivity measurements were performed by dissolving the complexes in DMSO with 10^{-3} M concentration and their molar conductivities were measured at room temperature. Infrared spectra were recorded on Perkin Elmer FTIR spectrophotometer. The ^{1}HNMR (300 MHz) and ^{13}CNMR (75.43 MHz) spectra were recorded on Bruker AM-250 spectrometer in $CDCl_3$ and DMSO solution using TMS as internal standard. UV Visible absorption spectra were recorded on UV-Vis Spectrophotometer UV-1700.

Synthesis of Ligands

1. 2-(((2-mercaptophenyl)imino)methyl)naphthalen-1-ol (**HL_1**)

2-hydroxynaphthaldehyde (1.72g, 10 mmol) dissolved in 20mL methanol was added to 2-aminothiophenol (1.25g, 10 mmol) dissolved in 10mL methanol. The two solutions were mixed and the mixture was refluxed with magnetic stirring for four hours. The product obtained was filtered, washed twice with methanol and diethyl ether dried and recrystallized from methanol. Bright yellow fluffy solid, (70%); m.p. 146-150 °C; FT-IR (cm^{-1}) υ; ν-OH 3259cm^{-1}(s)(disapp.), ν-=C-H 3053(v)cm^{-1}, ν-S-H 2736cm^{-1}(w)(disapp.), ν-C=N 1621cm^{-1}(s), ν-C=C arom. 1460cm^{-1} 1554cm^{-1}(m), ν-C-S sym. 816cm^{-1}(s), ν-C-S asym. 755cm^{-1}(s), aromatic o-disubst. 741cm^{-1}(s); ^{1}H-NMR (DMSO-d_6, 300 MHz) δ: 3.34 (s, 1H, SH), 6.6 (m, 2H, Ph.), 6.9 (m, 1H, Ph.), 7.1 (t, 1H,J=10.5 Hz Ph.), 7.2 (m, 1H, Ph.), 7.3 (m, 1H Ph), 7.35 (m,1H, Ph) 7.38 (m,1H, Ph), 7.78 (t, 2H, J=15.3 Hz), 10.54 (s, 1H, C=N), 15(s, 1H,OH); ^{13}C-NMR (DMSO-d_6, 300 MHz) δ: 63.96, 110.03, 114.76, 118.71, 119.74, 121.87, 123.14, 124.35, 125.96, 126.33, 127.03, 129.12, 129.17, 131.06, 132.91, 148.02 (Ph.), 154.51 (C=N); Anal. Calculations for $C_{17}H_{13}NOS$ %: C, 73.09; H, 4.69; N, 5.01; found: C, 73.0; H, 4.58; N, 4.99 (Scheme 1).

2. (E)-2-((4-chlorobenzylidene)amino)naphthalen-1-ol (**HL_2**)

Hydroxynaphthylamine (1.44g, 10 mmol) and 4-chlorobenzaldehyde (1.4g, 10 mmol) were dissolved in methanol (20 mL) and the mixture was refluxed for 6 hrs and then cooled to room temperature. The reaction mixture was filtered and the precipitate recrystallized from ethyl alcohol. Purple shiny ppt. (85%); m.p. 110-112 °C; FT-IR (cm^{-1}) υ; ν-OH 3365cm^{-1}, ν-C=N 1620cm^{-1}(s), ν-C=C arom.1594cm^{-1} ,1568cm^{-1}, 1487cm^{-1}(m), ν-C-N 1264 cm^{-1}(s), Arom. p-disubst. 839cm^{-1}(s), Arom. O-disubst. 775cm^{-1}(s), phenol 1089.26 cm^{-1}(s), ν-C-Cl 801cm^{-1} 575cm^{-1}(s). ^{1}H-NMR (DMSO-d_6, 300 MHz) δ: 7.5(m, 5H, Ph), 7.7 (d, 1H, J=8.4 Hz, Ph), 7.8 (t,1H, J=9.3 Hz, Ph), 7.9(d, 2H, J=8.4 Hz, Ph), 8.3(t, 1H, J=9.3 Hz, Ph), 8.5 (s, 1H, Ph.) 13.43 (s, 1H, OH): ^{13}C-NMR (DMSO-d_6, 300 MHz) δ: 112.67, 123.87, 125.84, 126.02, 126.10, 126.50, 127.69, 128.78, 129.16, 129.49, 130.14, 130.93, 133.93, 134.89 (Ph), 137.50 (C-Cl), 148.92 (C-OH), 158.87 (C=N); Anal. Calculations for $C_{17}H_{12}ClNO$ %: C, 72.47; H, 4.29; N, 4.97; found: C, 72.39; H, 4.20; N, 4.87 (Scheme 2).

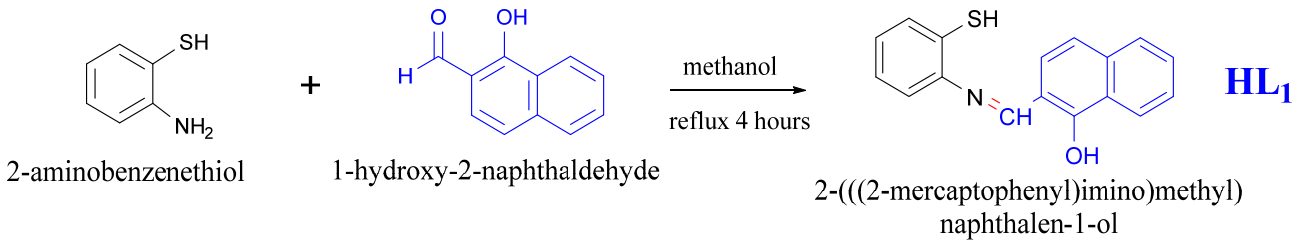

Scheme 1 – Synthesis of 2-(((2-mercaptophenyl)imino)methyl)naphthalen-1-ol (**HL_1**).

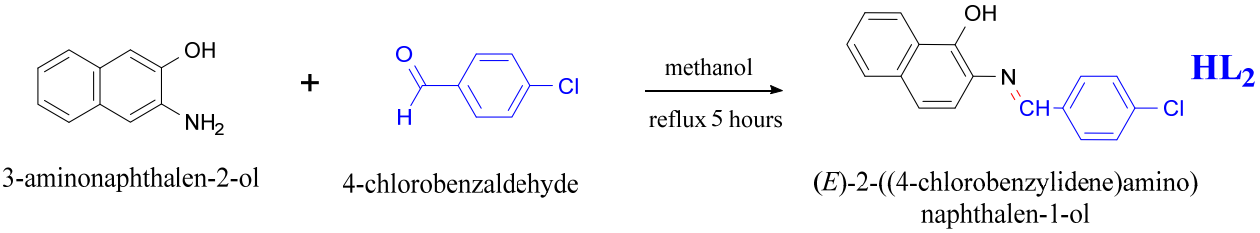

Scheme 2 – Synthesis of (E)-2-((4-chlorobenzylidene)amino)naphthalen-1-ol (**HL_2**).

3. 3-((4-chlorobenzylidene)amino)-4-hydroxy-5-nitrobenzenesulfonic acid (**HL_3**)

5-nitro-2-aminophenol-4-sulfonic acid (2.34g 10 mmol) was dissolved in methanol (20mL). 4-chlorobenzaldehyde (1.4g 10 mmol) was dissolved in 10 mL methanol. The solutions were mixed and the reaction mixture was refluxed for 4 hours with stirring. The solution was allowed to cool at room temperature. The excess solvent removed under reduced pressure, on rotary evaporator. The brown mass obtained was dissolved in methanol, slow evaporation yielded fine brown needle crystals of the Schiff base ligand. Brown ppt. (84%); m.p. 125-130 °C; FT-IR (cm^{-1}) υ; ν-OH 3379cm^{-1}(ν), ν-=C-H arom. 3027cm^{-1}(ν), ν-C=N 1626(s)cm^{-1}, nitro ν-N=O 1370cm^{-1}(s), 1568cm^{-1}(s), sulfonic acid ν-S=O 1205cm^{-1} 1276 cm^{-1}(s), phenol 1086 cm^{-1}(s), trisubst. Arom. 910cm^{-1}(w), p-disubst. Arom. 806.51cm^{-1}(s), ν-S-O 653cm^{-1}(s); ^{1}H-NMR (DMSO-d_6, 300 MHz) δ: 3.51 (s, 1H SO_3H) 6.9 (d, 1H, J=8.7 Hz Ph), 7.2 (t, 1H, J=4.2 Hz, ph) 7.4 (d, 2H, J=8.4 Hz, Ph) , 7.8 (d, 2H J=8.4 Hz, Ph), 8.5 (s, 1H, C=N), 10 (s, 1H, OH); ^{13}C-NMR (DMSO-d_6, 300 MHz) δ: 116.19, 116.23, 125.08, 128.81(2), 129.31(2), 130.11, 133.86, 135.82, 138.22, 150.96 (Ph.) 156.75 (C=N); Anal. Calculations for $C_{13}H_9ClN_2O_6S$ %: C, 43.77; H, 2.54; N, 7.85 found: C, 43.67; H, 2.49; N, 7.88 (Scheme 3).

Synthesis of Metal Complexes

$PdCl_2$ was converted to $K_2[PdCl_4]$ by reported procedure using KCl and $PdCl_2$ in 2:1 mole ratio and dissolving in distilled water. The mixture was left at room temperature for slow evaporation to yield fine shiny yellow green crystals of $K_2[PdCl_4]$. All the palladium complexes were prepared using the same procedure as given below (Scheme 4).

$K_2[PdCl_4]$ (0.326g 1mmol) was dissolved in methanol water mixture (2:1, 10mL). Ligand solutions were prepared by dissolving L_1 (0.558g 2mmol), L_2 (0.56g, 2mmol) and L_3 (0.712g, 2mmol) in 10mL methanol. The metal solution was added dropwise to corresponding ligand solutions. The mixture was stirred and heated at 50 °C for 10 minutes. Stirring was continued until complex was completely precipitated. The complex obtained was filtered, washed with methanol and air dried.

$Pd(L_1)_2$: (Color/state Yellow brown ppt.); (yield: 81%); (m.p; decomposed); FT-IR (cm^{-1}) □; ν-=C-H 3052 cm^{-1} (ν), ν-C=N 1601 cm^{-1} (s) (shifted -20 cm^{-1}), ν-C=C arom.1556 cm^{-1}, 1532 cm^{-1} 1461cm^{-1} (m), ν-C-S sym. 821cm-^{1} (s), ν-C-S asym. 755cm^{-1} (s), aromatic o-disubs. 743cm^{-1} (s), ν-Pd-S 568 cm-1 (s), ν-Pd-N 433cm^{-1} (s); ^{1}H-NMR (DMSO-d_6, 300 MHz) δ: 6.9 (1H, d, J=7.5 Hz), 7.1 (m, 2H, Ph.), 7.3 (m, 3H, Ph.), 7.5 (m, 1H Ph.), 7.7 (m, 2H Ph.), 8.0 (q, 1H, J=18.6 Hz), 9.7 (s, 1H C=N), 15.0 (s, 1H, OH) ^{13}C-NMR (DMSO-d_6, 300 MHz) δ: 110.02, 119.72, 120.55, 121.45, 124.30, 127.78, 128.03, 128.25, 128.63, 129.27, 129.50, 129.93, 133.18, 136.78, 145.72, 159.42 (Ph.), 165.38 (C=N) Anal. Calculations for $C_{34}H_{24}N_2O_2PdS_2$ %: C, 61.58; H, 3.65; N, 4.22; found: C, 61.50; H, 3.70; N, 4.30.

$Pd(L_2)_2$: (Color/state Brown ppt.) (yield 79%) (m.p; 253-255 °C); FT-IR (cm^{-1}) □; ν-=C-H 3053 cm^{-1} (ν), ν-C=N 1584 cm^{-1} (s) (shifted -36 cm^{-1}), ν-C=C arom.1514 cm^{-1},1454 cm^{-1} 1398 cm^{-1} (m), Arom. p-disubs. 849 cm^{-1} (s), Arom. O-disubs. 762 cm^{-1} (s), ν-C-Cl 789 cm^{-1},q ν- Pd-O 575 cm^{-1} (s), ν- Pd-N 473 cm^{-1} (s); ^{1}H-NMR (DMSO-d_6, 300 MHz) δ: 6.6 (d, 1H, J=7.5 Hz Ph.), 7.0 (d 1H J=8.1 Hz Ph), 7.1 (m, 2H, Ph), 7.3 (m, 3H Ph), 7.5 (m 1H Ph), 7.7 (d,1H, J = 7.5 Hz, Ph), 8.0 (t 1H J=13.8 Hz Ph) 8.6 (s 1H C=N) ^{13}C-NMR (DMSO-d_6, 300 MHz) δ: 107.85, 115.80, 121.28, 122.79, 124.06, 124.31, 125.93, 127.18, 128.25, 129.50, 130.45, 131.23, 134.63, 135.56, 145.13, 156.3, (Ph.) 169.21 (C=N) Anal. Calculated for $C_{34}H_{22}C_{l2}N_2O_2Pd$ %: C, 61.14; H, 3.32; N, 4.19; found: C, 61.09; H, 3.42; N, 4.22.

$Pd(L_3)_2$: (Color/state Yellow ppt.) (yield 79%) (m.p; decomposed); FT-IR (cm^{-1}) □; ν-C=N 1595 cm^{-1} (s) (shifted), ν-C=C arom. 1501 cm^{-1} ,1477 cm^{-1} 1446cm^{-1} (m), ν-nitro N=O 1385 cm^{-1} (s)1555 cm^{-1} (s), sulfonic acid ν-S=O 1136 cm^{-1} (s) 1268 cm^{-1} (s), phenol 1093 cm^{-1} (s), trisubs. Arom. 903 cm^{-1}(w), p-disubs. Arom. 805 cm^{-1} (s), ν-S-O 653 cm^{-1} (s), ν-Pd-O 541 cm^{-1} (s), ν-Pd-N 439 cm^{-1} (s); ^{1}H-NMR (DMSO-d_6, 300 MHz) δ: 3.34 (s, 1H, SO_3H), 6.3 (q, 1H, J=5.7 Hz, Ph), 6.4 (m, 1H, Ph) 6.5 (q, 1H, J = 1.5 Hz, Ph) 6.7 (d, 1H, J=2.4 Hz), 6.8 (t, 1H, J=9.3 Hz, Ph), 7.0(d, 1H, J=12 Hz, Ph), 9.2 (s, 1H, C=N); ^{13}C-NMR (DMSO-d_6, 300 MHz) δ: 113.65, 115.46, 115.54, 117.19, 117.93, 123.30, 125.72, 127.89, 131.82, 138.89, 143.27 168.07 (Ph.) 169.21 (C=N); Anal. Calculations for $C_{26}H_{16}C_{l2}N_4O_{12}PdS_2$ %: C, 38.18; H, 1.97; N, 6.85; found: C, 38.28; H, 1.87; N, 6.75.

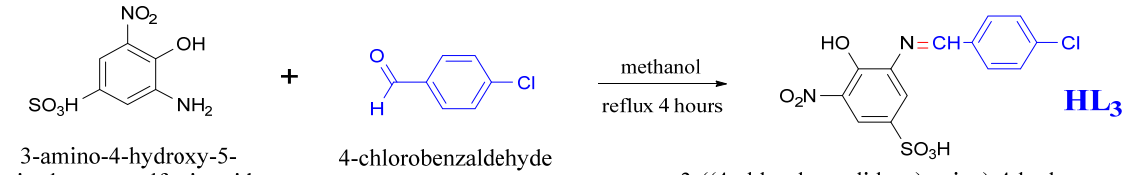

3-amino-4-hydroxy-5-nitrobenzenesulfonic acid

4-chlorobenzaldehyde

3-((4-chlorobenzylidene)amino)-4-hydroxy-5-nitrobenzenesulfonic acid

Scheme 3 – Synthesis of 3-((4-chlorobenzylidene)amino)-4-hydroxy-5-nitrobenzenesulfonic acid (**HL_3**).

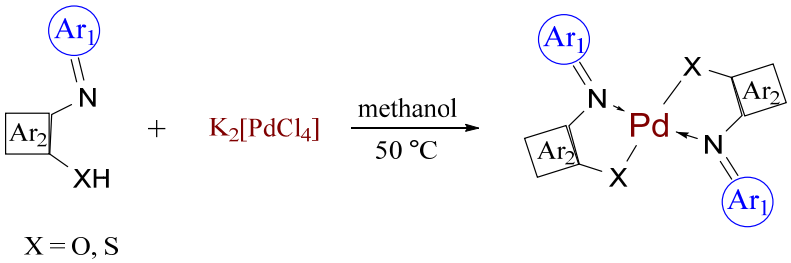

X = O, S

Scheme 4 – General synthesis of metal complexes.

UV-Visible Spectroscopy

UV-Visible spectrum of the complex was recorded on UV-1800 Shimadzu spectrometer within the wavelength range of 190-800 nm with lower cut off at 220 nm. 1mM solution of the complex was prepared in DMSO at room temperature. Bands in the region of 400 nm to 800 nm were assigned to d-d transitions and in the region of 220 nm to 380 nm assigned to $\pi\rightarrow\pi^*$, $n\rightarrow\pi^*$ and ligand to metal charge transfer transitions.

DNA Binding Activity Studies

The binding interaction between metal complexes and DNA was studied using electronic absorption method and UV-Vis Spectrophotometer UV-1700 in the wavelength range 200-800 nm. Calf Thymus DNA was stirred at 4 ºC. DNA stock solution was prepared with buffer solution (50 mM tris HCl at pH 7.2). The concentration of CT-DNA (calf thymus-deoxyribonucleic acid) per nucleotide was determined spectrophotometrically by using an extinction coefficient of 6600 M^{-1} cm^{-1} at 260 nm. Concentrated stock solutions of the ligand and complexes were prepared in DMSO and diluting suitably to the required concentration for all the compounds used to conduct absorption experiments.

Bacterial Inhibition Studies

The synthesized compounds were screened for their antibacterial activity against Gram negative organisms which include *Escherichia coli*, *Salmonella*, *Klebsiella* and *Pseudomonas* by disk diffusion technique.[11] They were grown routinely overnight in a nutrient broth (Merck) at 37 ºC. A disc diffusion assay was employed for the evaluation of antibacterial activity. 6 mm filter paper discs were impregnated with 20-100 mg/mL concentrations of test compounds in DMSO and were allowed to remain at 37 ºC till complex diluents evaporation and kept under refrigeration before antibacterial activity was assessed. 1 cm^3 of a 24 h broth culture containing 10^6 CFU/cm^3 was placed in sterile Petri-dishes. Molten nutrient agar (15 cm^3) maintained at 45 ºC was then poured into the Petri-dishes and allowed to solidify. 6 mm filter paper discs impregnated in the test solutions were placed in the centre of each plate along with the DMSO disc and standard drug (Kanamycin) disc which acted as positive control. DMSO was used as solvent and also for negative control. DMSO was found to have no antimicrobial activity against any of the test organisms. The release of drug into surrounding agar medium shown by growth inhibition of microorganisms was evaluated. The growth inhibitory effect was determined by measuring the zone of growth inhibition around the disc.

α-Glucosidase Inhibition Study

α-Glucosidase enzyme inhibition assay was performed by employing previously reported procedure with modifications.[12] Solution of commercial α-glucosidase enzyme (1unit/ml) and the substrate (20 mM) p-nitrophenyl-α-D glucopyranoside (PNG) was prepared in 50 mM phosphate buffer (pH 6.8). 96-Well plates were used to perform the assay in triplicates with Acarbose as control. The assay was performed by mixing 25 µL of PNG, 65 µL of buffer and 5 µL of enzyme along with 5 µL of complex solution in DMSO with final concentrations of 200, 100 and 50 ppm, respectively. These mixtures were incubated at 35 °C for 30 min. After incubation, 0.5 mM sodium bicarbonate (100 µl) was added as stopping reagent. Percentage inhibition was calculated by the given formula and taking absorbance (Abs.) at 405 nm with microplate reader (BioTek Elx-800). IC_{50} value was calculated by using GraphPad Prism 5[13]. Percentage inhibition = [(Abs. of control – Abs. of sample)/ Abs. of control] ×100.

RESULTS AND DISCUSSION

FT-IR Analysis

FTIR spectroscopy is an important tool for identifying the coordinating nature of the ligand with the metal ions. The FITR spectrum provides valuable information regarding the nature of the functional group attached with the metal ion in the synthesized Schiff base metal complexes. The FTIR spectra of the three ligands and their palladium (II) complexes have been shown in Table 1. The synthesized ligands and complexes were characterized based on C=N (azomethine), M-O, M-S and M-N absorption bands. FTIR spectra of the compounds were recorded in the range 400-4000cm^{-1} to indicate the regions of absorbing vibrations. The IR spectra of the complexes were compared with those of free ligands in order to determine the coordination sites involved in chelation. The broad peaks in high frequency region of L_1 appearing at 3295 cm^{-1} and 2736 cm^{-1} are due to OH and SH stretching vibrations. Similarly, the peaks at 3365 cm^{-1} and 3379 cm^{-1} in spectra of L2 and L3 are due to OH stretching vibrations. These peaks disappear in the spectra of the complexes which suggest the deprotonation of OH and SH groups to form bonds with palladium metal. This is further supported by the appearance of new bands at 512-568 cm^{-1} in low frequency region of metal complex spectra which are due to the Pd-O and Pd-S stretching vibrations. The peaks at 1601 cm^{-1},1584 cm^{-1} and 1595 cm^{-1} in Schiff base ligands is assigned to C=N stretching vibration[20]. The band shows shift by 20-30 cm^{-1} in spectra of complexes (observed at 1621 cm^{-1}, 1620 cm^{-1} and 1626 cm^{-1}), which indicates the participation of azomethine nitrogen in coordination with metal. New bands at 512-568 and 432-448 cm^{-1} which do not exist in the free ligand are assigned to ν-(M-O), ν-(M-S) and ν-(M–N) vibrations.

$Pd(L_1)_2$: The important peaks in the spectrum of the ligand are 3259 cm^{-1} for OH stretching vibration, a band at 3053 cm^{-1} for aromatic C-H stretch. A weak band at 2736 cm^{-1} is assigned to SH which disappears in spectrum of complex. C=N azomethine band appears at 1621 cm^{-1} which is shifted downfield to 1601 cm^{-1} in spectrum of complex indicating the participation of azomethine nitrogen in complexation. Aromatic C=C bands appear at 1460cm^{-1}, 1554 cm^{-1}. ν C-S sym. and ν C-S asymmetric vibration appear at

821cm^{-1} and 755cm^{-1}. Aromatic o-substituted sharp band appear at 743 cm^{-1}. New bands appearing in low frequency regions of metal complexes at 432cm^{-1} and 568 cm^{-1} are assigned to M-N and M-S respectively.

$Pd(L_2)_2$: The characteristic bands appearing at 1620 cm^{-1} are assigned to C=N azomethine stretching vibration. Aromatic C=C stretching vibrations appear at 1568 cm^{-1}, 1487 cm^{-1} and 1406 cm^{-1}. Strong band at 839 cm^{-1} is due to aromatic *para*-disubstituted and a strong band at 775 cm^{-1} is due to o-substitution. C-Cl stretching bands appear at 801 and 575 cm^{-1}.

The spectrum of complex aromatic C-H stretch appears at 3053 cm^{-1}. The characteristic C=N band is shifted from 1620 cm^{-1} to 1584 cm^{-1}. The hydroxyl band in ligand appearing at ν-OH 3365 cm^{-1} has disappeared in spectrum of complex, C=C band of aromatic appears at 1514 cm^{-1}, 1454 cm^{-1} and 1398 cm^{-1}. P-disubstituted aromatic band appears at 849 cm^{-1}. C-Cl stretching band appears at 575 cm^{-1} and 789 cm^{-1}. Strong band for aromatic o-substitution appear at 762.15 cm^{-1}. Two new bands appearing at low frequency regions at 512 cm^{-1} and 448 cm^{-1} are assigned to Pd-O and Pd-N respectively.

$Pd(L_3)_2$: The main regions of absorption are 3379 cm^{-1} for OH stretching vibration, a band at 3027 cm^{-1} for =C-H aromatic stretching vibration. The band at 1626 cm^{-1} is for C=N stretching vibration. N=O stretching vibration appears at 1370 cm^{-1} and 1568 cm^{-1}. Aromatic C=C bands appear at 1478 and1492 cm^{-1}. S=O stretch at 1205.67 cm^{-1} and 1276 cm^{-1}. S-O band at 653 cm^{-1}. Trisubstituted aromatic band appears at 910 cm^{-1}. Aromatic p-disubstituted sharp band appears at 806 cm^{-1}. Bands for C-Cl stretching vibrations appear at 697 and 761 cm^{-1}.

In the spectrum of complex the OH band at 3379 cm^{-1} has disappeared. C=N band is shifted from 1626 cm^{-1} to 1595 cm^{-1}. New bands appear in the region 541 cm^{-1} and 439 cm^{-1} are assigned to Pd-O and Pd-N respectively.

Multi nuclear (^{1}H and ^{13}C) NMR analysis

^{1}HNMR spectra of the compounds were recorded in DMSO or $CDCl_3$ solvents. The spectra are shown in Tables 2 and 3. The spectra of the ligands and their complexes were compared to indicate the position of shifted bands and disappearing bands to identify the structure of complex. The chemical shifts (δ in ppm) of various protons in ligand and metal complexes are reported below.

$Pd(L_1)_2$: ^{1}HNMR spectrum of L_1 shows SH proton peak at 3.34 ppm azomethine proton peak at 10.54 ppm OH proton at 15 ppm and aromatic protons between 6.6-7.78 ppm. A total of 24 protons for two ligands are shown in the spectrum of complex with aromatic proton appearing between 6.9-8.0 ppm, C=N proton at 9.7 ppm and OH proton appearing at 15 ppm. ^{13}CNMR shows 17 peaks. Azomethine and phenolic carbon peaks appear at 154 and 148 ppm which are shifted downfield at 159.42 and 165.38 ppm in spectra of complex.

$Pd(L_2)_2$: azomethine proton at 8.6 ppm. Aromatic protons appear between 6.6-8.0 ppm. ^{13}CNMR shows 17 peaks at azomethine carbon which appear at 169.21 ppm.

$Pd(L_3)_2$: Ligand shows OH peak 10 ppm, azomethine proton at 8.5 ppm and aromatic protons between 6.9-7.8 ppm. In the spectrum of complex OH peak has disappeared showing it is used in complexation with metal. Azomethine proton is shifted downfield to 9.2 ppm which indicates the involvement of azomethine nitrogen in complexation. Aromatic protons appear between 6.3-7.0 ppm in the spectrum of complex.

The results show a successful coordination of ligands through azomethine nitrogen and phenolic oxygen. Palladium forms square planar diamagnetic complexes in +2 oxidation states (Figure 1). The conclusions drawn from these studies lend further support to the mode of bonding discussed in their IR spectra.

Electronic Spectra

The electronic spectra of the ligand and their complexes have been measured in DMF solution between 200-800 nm at room temperature. Electronic spectra of the three Schiff base ligands and their palladium (II) complexes have been shown in Table 4. In the spectra of the Schiff base ligand, the absorption bands observed at 280 nm region were assigned to a benzene π-π* transition and the bands at 390 nm assigned to n-π* transition associated with the azomethine chromophore (-C=N). The new bands observed near 390-450 nm can be assigned to L→M charge transfer band. The spectra of the ligands and complexes are shown in Figure 2. In the $[Pd(NA4CBA)_2]$ complex the two bands at (569 and 533nm) were attributed to (d-d) electronic transition $[^3A_2(F) \rightarrow {}^3T_1(F)]$ and $[^3A_2(F) \rightarrow {}^3T_2(F)]$ respectively suggesting a square planar geometry about palladium atom. Similarly, spectra of [Pd(2HN2ATP)2] and $[Pd(NAPSA4CBA)_2]$ were showing peaks at (733, 381, 317 and 265 nm) as well as (734, 673 and 301nm) corresponding to the electronic transitions of $[^3A_2(F) \rightarrow {}^3T_1(F)]$ and $[^3A_2(F) \rightarrow {}^3T_2(F)]$ and charge transfer,

suggesting a square planar geometry for the palladium complexes.

DNA Binding study

The alteration in absorption spectrum of drug upon the addition of an increasing amount of DNA is one of the most widely used methods for investigating the characteristic DNA binding modes of antibacterial drugs. Compound can bind to DNA through both intercalation and non-intercalation like covalent bonding or groove binding. As a result of intercalation, a strong interaction between an aromatic group and base pairs of DNA results in the hypochromic effect with small blue or red shift. On the other hand, the binding mode of groove binding shows titration spectra with hyperchromic effect involving the binding of compound to the outer or inner spaces of DNA. The magnitude of hypochromic effect is related to the strength of interaction between compound and DNA. The capability of binding strength of compound to DNA can be shown in the term of binding constant, K_b. K_b was determined from the slope of the plot Ao/A-Ao *vs.* 1/[DNA] $(\mu M)^{-1}$ and was used for the calculation of ΔG using the equation $\Delta G = -RT \ln K_b$. Therefore, in order to obtain evidence for the possibility of binding each complex, the samples were subjected to UV-visible analysis (Figure 2a-2b).

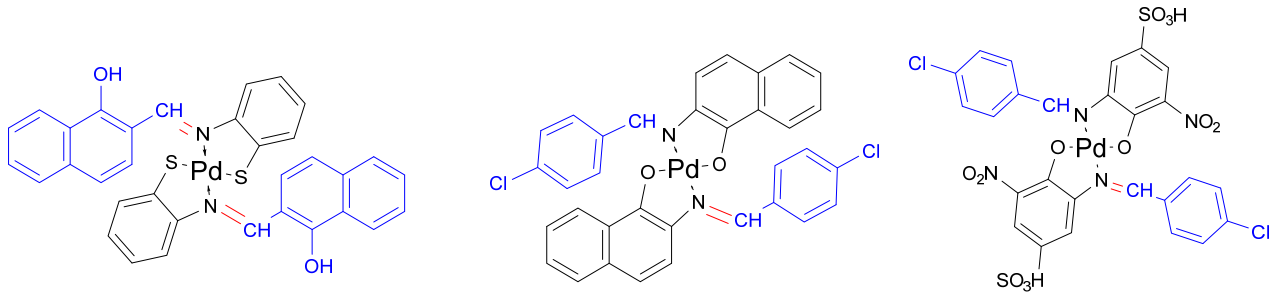

$Pd(L_1)_2$ $Pd(L_2)_2$ $Pd(L_3)_2$

Fig. 1 – Proposed structures of synthesized metal complexes.

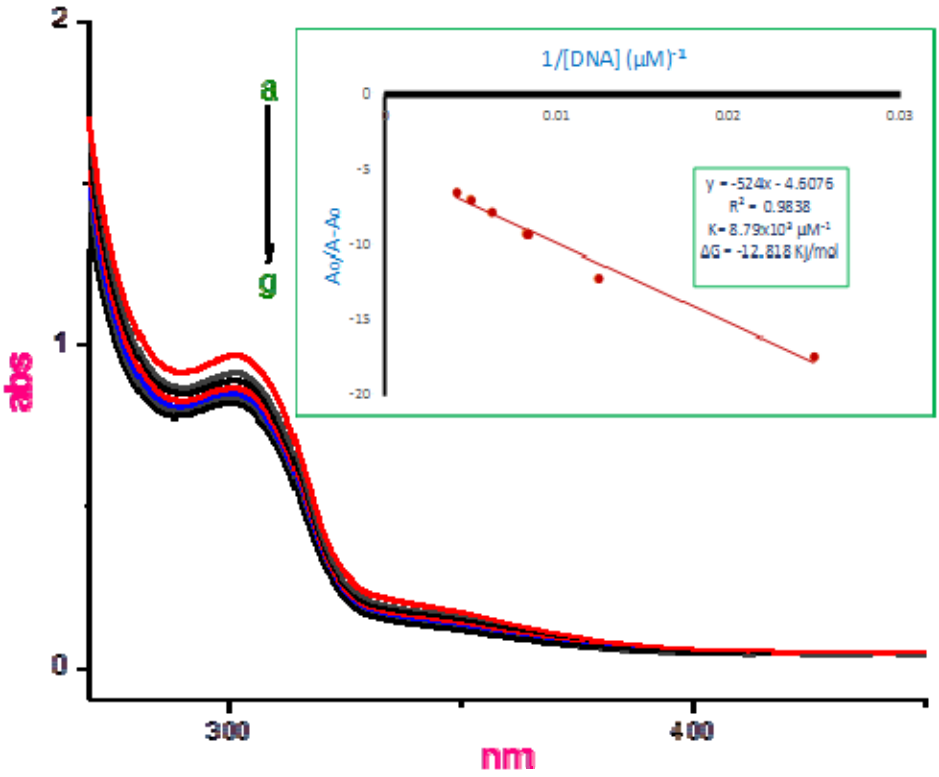

Fig. 2a – Absorption spectrum of $Pd(L_1)_2$ in varied conc. of DNA and determination of Gibb's free energy (ΔG) and binding constant (K).

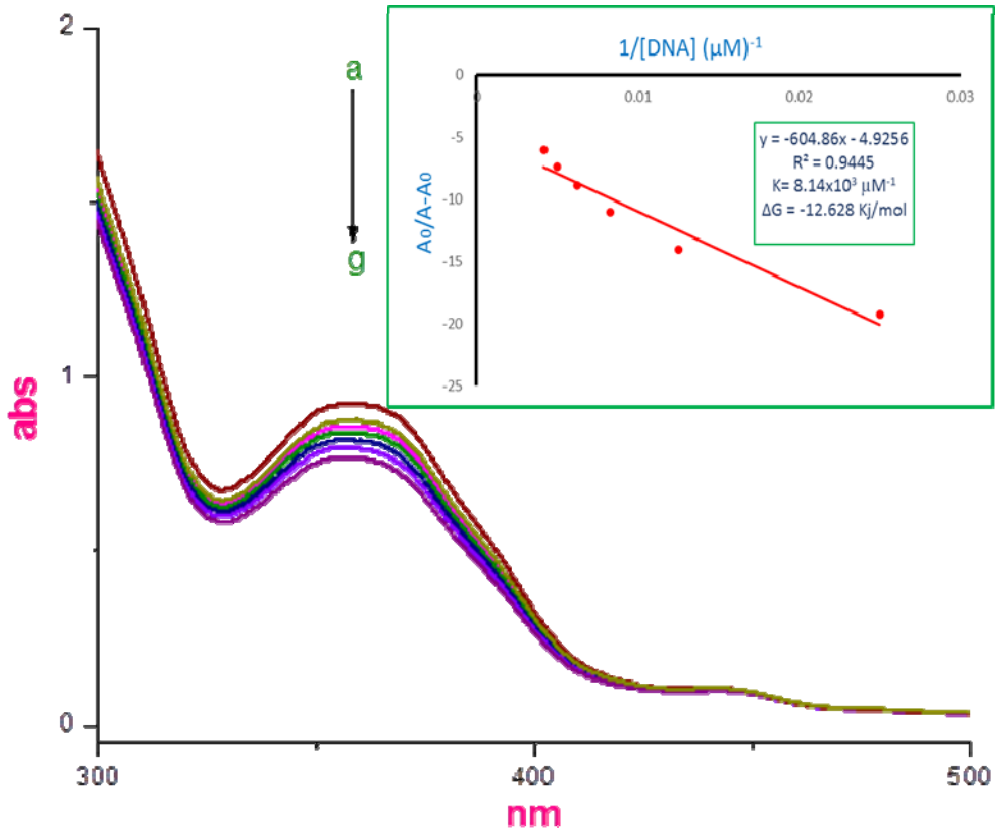

Fig. 2b – Absorption spectrum of $Pd(L_2)_2$ in varied conc. of DNA and determination of Gibb's free energy (ΔG) and binding constant (K).

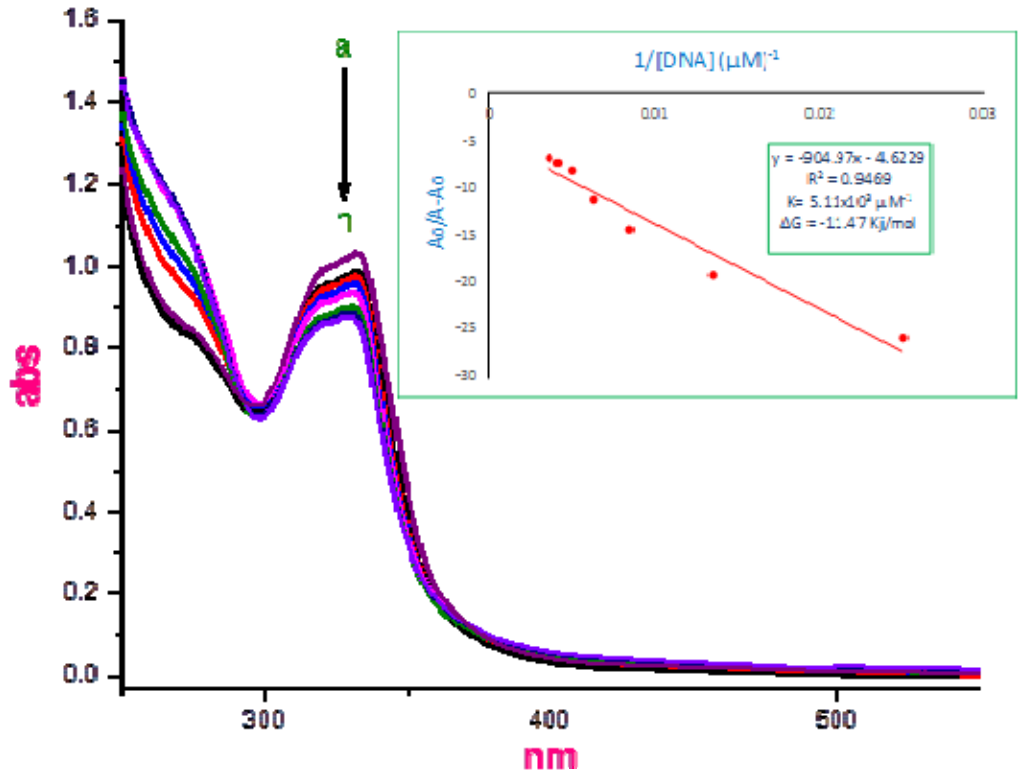

Fig. 2c – Absorption spectrum of $Pd(L_3)_2$ in varied conc. of DNA and determination of Gibb's free energy (ΔG) and binding constant (K).

Antibacterial activity

The probable mechanism of antibacterial activity is related to the ability of Schiff bases, ligands and complexes to penetrate into the outer lipid layer of the cell membrane and to extend into the cell wall. Then complexes can induce the cell wall damage, leading to the conformational changes and terminate the bacterial life cycle. The mechanism of action of drugs can be described on the basis of chelation theory[14], which suggests that on chelation of ligand to the metal, the polarity of the metal ion is reduced to a great extent due to the overlap of the ligand orbital with the metal orbital and there is partial sharing of the positive charge of the metal ion with donor atom and increases the delocalization of π-electrons over the chelate ring. Thus, chelation enhances the lipophilic character of the central metal atom, which subsequently favors its permeation through the lipid layers of the cell membrane and enhances the penetration of the complexes into the lipid membrane, thereby blocking the metal binding sites in the enzymes of the microorganism. Many *in vitro* studies have shown the inhibition of enzyme activities in the presence of transition metal complexes.[15] mechanism of action of antimicrobial agent can be categorized on the basis of the structure of bacteria and function that is affected by the agent. Inhibition of enzymes can disturb the respiration process, cell homeostasis and thus block the synthesis of proteins which restricts the further growth of the organisms (Figure 3).

α-Glucosidase Inhibition Study

α-Glucosidase is present in the brush border of small intestine and it catalyzes the last glucose releasing step in starch digestion. By regulating its action through α-glucosidase inhibitor is an attractive approach for controlling blood glucose levels for the treatment of Type II diabetes in modern era of medicine.[16] In the present study, α-glucosidase enzyme inhibition activity of the compounds was determined by using PNG as a substrate, where Acarbose (IC_{50} 20.29 µM) served as positive control (Figure 4). The results showed that the compound exhibited enzyme inhibition activity in dose dependent manner with IC_{50} value 13.1 µM. The significant enzyme inhibition activity of the compound represented the positive potential of the complex to be used as anti-diabetic agent.[17]

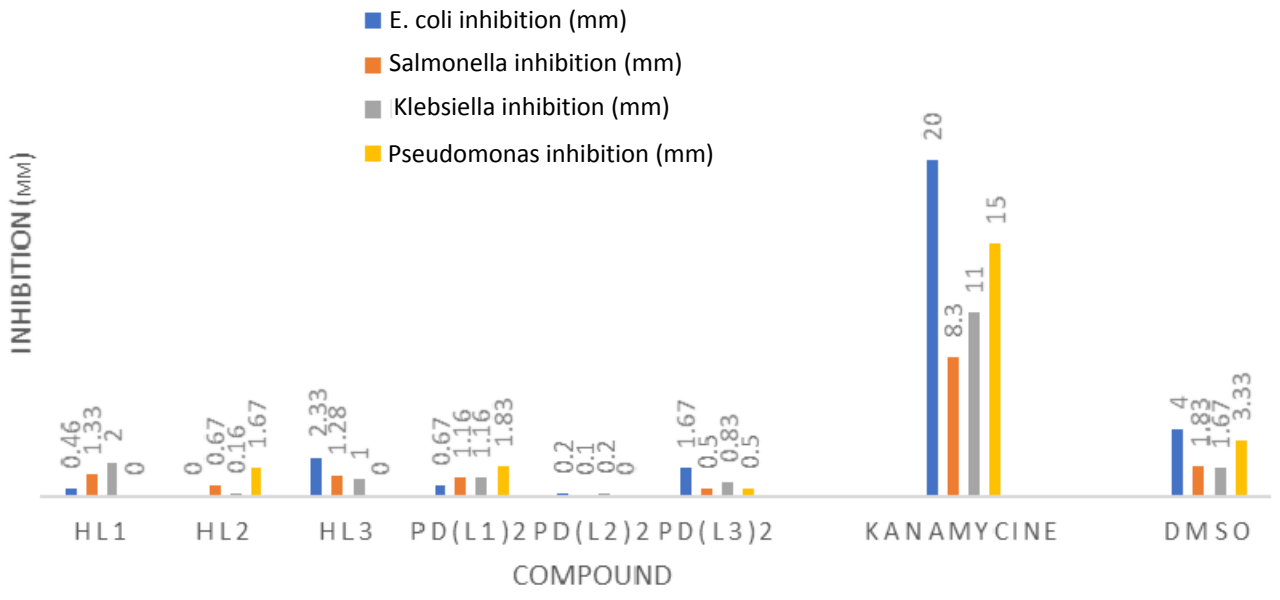

Fig. 3 – Antibacterial activity of synthesized compounds.

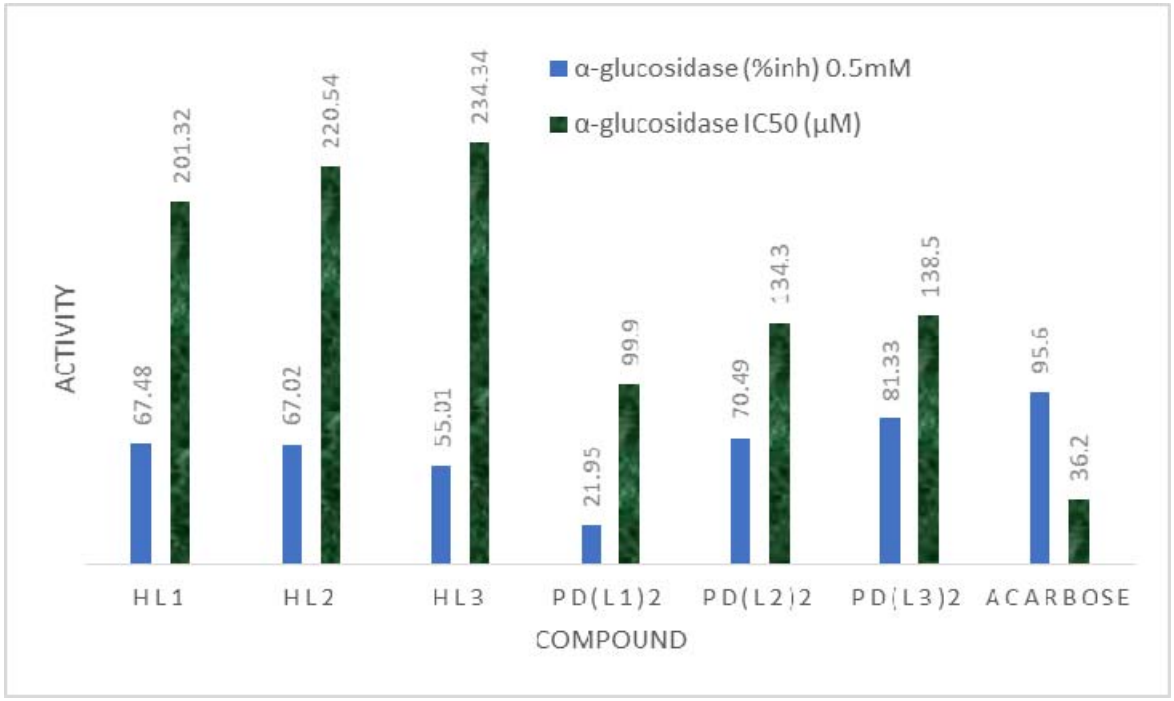

Fig. 4 – α-Glucosidase inhibition activity of synthesized compounds.

CONCLUSION

The synthesis and characterization of palladium (II) compound as the antibacterial drug in the presence of a nitrogen donor Schiff base has been achieved. The structural conformation of drug through UV, IR and NMR spectral data reveals the combination of ligand and Pd (II) as 1:2 square planar chelate complexes. The *in vitro* antibacterial activity of drug has been validated against four-gram negative strains of bacteria via paper disc diffusion assay and compared with standard Kanamycin. The synthesized drug displayed moderate activity. In order to determine the hypothesized mechanism on antibacterial activity, the DNA binding experiment by UV titration was performed. The result revealed that drug could bind to calf thymus -DNA through intercalation. Hence all the data presented in this paper reflects that synthesized complexes can provide a useful foundation in the future to design some metal-based drugs.

REFERENCES

1. Z. L. You, H. L. Zhu and W. S. Liu and *Z. Anorg. Allg. Chem.*, **2004**, *630*, 1617-1622.
2. A. Golcu, M. Tumer, H. Demirelli and R. A. Wheatley, *Inorg. Chim. Acta*, **2005**, *358*, 1785-1797.
3. S. Verma, A. K. Mishra and J. Kumar, *Acc. Chem. Research*, **2009**, *43*, 79-91.
4. K. P. Carter, A. M. Young and A. E. Palmer, *Chemical Reviews*, **2014**, *114*, 4564-4601.
5. K. Karlin, A. Zuberbühler, J. Reedijk and E. Bouwman, "Bioinorganic Catalysis", by J. Reedijk and E. Bouwman, Marcel Dekker, New York 1999, p. 469-534.
6. J. M. Gutteridge, G. J. Quinlan and P. Kovacic, *Free Radical Res.,* **1998**, *28*, 1-14.
7. M. Galanski, *Recent Pat. Anticancer Drug Discov.,* **2006**, *1*, 285-295.
8. E. Gao, C. Liu, M. Zhu, H. Lin, Q. Wu and L. Liu, *Anti-Cancer Agents Med. Chem. (Formerly Curr. Med. Chem.-Anti-Cancer Agents)* **2009**, *9*, 356-368.
9. K. S. Prasad, L. S. Kumar, S. Chandan, R. N. Kumar and H. D. Revanasiddappa, *Spectrochim. Acta Part A: Molecul. Biomolecul. Spectroscopy,* **2013**, *107*, 108-116.
10. A. Garoufis, S. Hadjikakou and N. Hadjiliadis, *Coord. Chem. Rev.,* **2009**, *253*, 1384-1397.
11. P. E. Coudron, *J. Clinic. Microbiol.*, **2005**, *43*, 4163-4167.
12. S. Ferheen, Aziz-Ur-Rehman, N. Afza, A. Malik, L. Iqbal, M. Azam Rasool, M. Irfan Ali and R. Bakhsh Tareen, *J. Enzyme Inhib. Med. Chem.*, **2009**, *24*, 1128-1132.
13. V. Gorun, I. Proinov, V. Băltescu, G. Balaban and O. Bârzu, *Anal. Biochem.* **1978**, *86*, 324-326.
14. A. Albert, "Selective Toxicity: the physico-chemical basis of therapy", Springer Science & Business Media: Adrien Albert, Springer Netherlands, 2012, p. 21-55.
15. D. Mohanambal and S. Arul Antony, *Res. J. Chem. Sci.*, **2014**, *4*, 1-6.
16. K. K. Naik, S. Selvaraj, N. Naik, *Spectrochim. Acta Part A: Molecul. Biomolec. Spectroscopy,* **2014**, *131*, 599-605.
17. I. Tripathi, M. M. Kumar, K. Arti, M. Chinmayi, T. Ruchita, S. L. Kant, P. K. Bihari, *Res. J. Chem. Sci.*, **2013**, *3,* 54-59.